*American Mineralogist, Volume 76, pages 1533–1546, 1991*

# Hydrous species in zircon

**James A. Woodhead**
Department of Geology, Occidental College, Los Angeles, California 90041, U.S.A.
**George R. Rossman**
Division of Geological and Planetary Sciences, California Institute of Technology, Pasadena, California 91125, U.S.A.
**Andrew P. Thomas***
Department of Geology, Occidental College, Los Angeles, California 90041, U.S.A.

## Abstract

A survey of hydrous species in zircon from a number of localities with a range of occurrences and structural states was carried out using infrared spectroscopy and electron microprobe analysis. Stepwise heating experiments on a crystalline and a nearly metamict zircon were also performed. The region of IR spectra of OH-bearing crystalline zircon from 4000 to 2500 $cm^{-1}$ exhibits anisotropic OH bands resulting from at least three OH sites, one at vacant tetrahedra and two that may be at Si-occupied tetrahedra. One site associated with Si-occupied tetrahedra is the most important, producing IR absorption bands at ~3420 $cm^{-1}$ ($\mathbf{E} \| \mathbf{c}$) and ~3385 $cm^{-1}$ ($\mathbf{E} \perp \mathbf{c}$). OH may be introduced during crystal growth by a coupled substitution of the form $[M^{3+} + H^{+}] \leftrightarrow [Zr^{4+}]$. The sites at vacant tetrahedra account for considerably less OH, producing relatively weak IR absorption bands at ~3510 $cm^{-1}$ ($\mathbf{E} \| \mathbf{c} > \mathbf{E} \perp \mathbf{c}$). OH may be introduced during crystal growth by the hydrogrossular substitution of the form $[4(OH)^{-}] \leftrightarrow [(SiO_4)^{4-}]$. An additional OH band at ~3270 $cm^{-1}$ appears to be associated with an occupied tetrahedron. Heating experiments produced two more OH environments and indicate that H can migrate among the sites at high temperatures. Some crystalline samples are entirely free of OH.

IR spectra of metamict zircon exhibit broad, asymmetric, isotropic OH bands similar to $H_2O$ bands, but the absence of the $H_2O$ bending-mode band indicates that OH is the dominant hydrous species present. IR spectra of partially metamict zircon samples retain some anisotropy. The breadth of their OH bands is a function of degree of metamictization.

The maximum OH observed in any metamict or partially metamict zircon sample was approximately 0.1 wt%, expressed as $H_2O$. Such OH is probably secondary. The maximum primary OH observed is ~0.05 wt% in partially metamict zircon from a hydrothermal vug. Crystalline crustal zircon contains more than an order of magnitude less OH. The maximum OH content observed in crystalline zircon, ~0.01 wt%, is in a mantle zircon sample from a kimberlite, suggesting high activity of $H_2O$ in the mantle.

Additional OH is present in some metamict and partially metamict zircon samples in the form of inclusions of hydrous silicates such as kaolinite. Fluid inclusions containing $H_2O$ occur in some samples. This may be a partial explanation of the high $H_2O$ contents reported for some radiation-damaged zircon based on loss-on-heating measurements.

## Introduction

Zircon is considered to be an anhydrous mineral, but a number of studies have reported the presence of a hydrous component in natural samples (Frondel, 1953; Frondel and Collette, 1957; Coleman and Erd, 1961; Mumpton and Roy, 1961; Krstanovic, 1964; Caruba et al., 1985; Woodhead et al., 1991). The hydrous species has been attributed to $H_2O$ or OH (or a combination of the two) in amounts up to 16.6 wt%—just over 50 mol% $H_2O$ (Coleman and Erd, 1961). In every case, the zircon varieties with reported $H_2O$ (such as cyrtolite, malacon, ribierite, and naegite) have been found to be metamict or nearly so. Zircon becomes metamict as a result of accumulated damage to the crystal structure caused by radioactive decay of U and Th, which substituted for Zr during initial crystallization. Such radiation damage expands the crystal lattice and decreases crystallinity, ultimately producing an amorphous glass that may be open to the infiltration of secondary hydrous species (Mumpton and Roy, 1961) into the disturbed structure or along cracks and grain boundaries. Hydrous species in cracks or at

* Present address: 2265 Via Cascabel, Escondido, California 92027, U.S.A.

0003–004X/91/0910–1533$02.00

grain boundaries cannot be considered true hydrous components of zircon, although they may be difficult to avoid when measuring $H_2O$ by weight loss on heating.

Ever since Holland and Gottfried's (1955) classic study of alluvial zircon from Sri Lanka, that suite has been considered prototypical of natural zircon with a wide range of crystallinities. In a detailed IR spectroscopic study of Sri Lanka zircon, Woodhead et al. (1991) found that the only detectable hydrous species is OH and that actual OH contents are quite low, approximately 0.03 wt% or less, expressed as $H_2O$. Zircon from Sri Lanka is thought to have formed in granulite pegmatites but has not been found in situ (Munasinghe and Dissanayake, 1981; Kröner et al., 1987). It is free of OH over the full range of structural states from crystalline to nearly metamict. OH does occur in metamict grains or zones, where it is uncorrelated with U content. Apparently, Sri Lanka zircon was initially anhydrous and took up OH only after becoming metamict. The amount of OH incorporated must depend on the conditions in the environment subsequent to metamictization and must be unrelated to $H_2O$ present in the original crystallization environment.

Studies of synthetic zircon have demonstrated that OH can be incorporated into the structure of crystalline samples (Frondel and Collette, 1957) by the substitution $[4(OH)^-] \leftrightarrow [(SiO_4)^{4-}]$. The resulting Si-deficient, hydroxylated zircon is analogous to hydrogrossular. Caruba et al. (1985) have reported samples with up to 81% of the $[(SiO_4)^{4-}]$ replaced by $[4(OH)^-]$. Their IR spectra exhibit a characteristic OH-stretching band at 3515 $cm^{-1}$ that decreased in intensity upon heating in air. Because no crystalline OH-bearing zircon has been reported in nature and synthetic hydroxylated zircon is apparently less stable than anhydrous zircon, the relation between the speciation of OH in synthetic and natural zircon remains to be established.

Several recent studies have shown that OH is a common trace constituent in silicates normally considered anhydrous (Aines and Rossman, 1985; Rossman et al., 1989; Beran et al., 1989; Lager et al., 1989; Skogby and Rossman, 1989). Minerals such as quartz, feldspars, pyroxenes, sillimanite, and garnets exhibit sharp IR absorption bands characteristic of OH structurally incorporated at the time of growth. Some of these silicates exhibit several OH bands, indicative of multiple sites or orientations of OH. OH in pyroxenes (Skogby and Rossman, 1989) and $H_2O$ in nepheline (Beran and Rossman, 1989) have been observed to change orientation in the course of heating experiments, indicating that the location of the hydrous species in some silicates is mutable. Rossman and Aines (1991) have found that the IR spectra of garnets with trace OH contents do not resemble those of hydrogrossular, suggesting that the speciation of trace OH in those garnets is not the same as in Si-deficient hydrogrossulars where the substitution $[4(OH)^-] \leftrightarrow [(SiO_4)^{4-}]$ occurs at the tetrahedral sites. This raises the possibility that in zircon, whose structure is somewhat similar to garnet (Robinson et al., 1971), trace amounts of OH may not follow the hydrogrossular substitution model even though such Si-deficient zircon can be produced in the laboratory.

We undertook a general survey of zircon to detect whether crystalline zircon can incorporate hydrous species and whether metamict ones can be anhydrous, as well as to determine the extent of OH incorporation, the variety of OH orientations and sites, the thermal stability of such sites, the relationship between synthetic hydroxylated zircon and natural zircon with a hydrous component, and the relationship between metamictization and hydrous species.

## Experimental details

Natural zircon samples from several localities with a range of occurrences, parageneses, habits, colors, and structural states (Table 1) were studied by IR spectroscopy and analyzed by electron microprobe. Roughly half the samples were free of inclusions; two had inclusions in cracks that could be avoided by the IR beam; several others contained dusty, birefringent inclusions in numerous cracks or randomly distributed throughout; the Sonora zircon contained prismatic apatite(?) inclusions; and the Bedford "cyrtolite" was an intergrowth of zircon, quartz, and monazite. A pure $ZrSiO_4$ synthetic zircon (Chase and Osmer, 1966) was studied for comparison. Heating experiments were conducted on two samples, one crystalline and the other nearly metamict. Each sample was heated for 1 h periods at about 100 °C intervals in an open furnace. Following each stepwise annealing period, polarized IR spectra were obtained at room temperature.

A Nicolet 60SX FTIR spectrometer was used to obtain IR spectra of most zircon samples. Polarized absorption spectra in the range 9500–1850 $cm^{-1}$ were obtained on doubly polished, single-crystal zircon plates cut parallel to the c-axis. A Perkin-Elmer model 180 double-beam grating infrared spectrometer was used to obtain spectra in the range 4000–1400 $cm^{-1}$ for the metamict zircon heating experiment. The absorption bands observed for each sample between 4000 and 2500 $cm^{-1}$ are listed in Table 2.

A JEOL 733 electron microprobe was used for chemical analyses of the polished, single-crystal zircon plates. Proportions of 13 elements were determined. The standards used for the analyses were mineral samples or synthetic oxides—Al and Ca, anorthite; Si, Zr, and Hf, Pacoima Canyon pegmatite zircon; P, Durango fluorapatite; Ti, rutile; Mn, manganese olivine; Fe, fayalite; Y, synthetic $Y_2O_3$; Nb, synthetic NbO; Th, synthetic $ThO_2$; and U, synthetic $UO_2$. X-ray peaks for the minor and trace elements were chosen to avoid interference by those of the major elements as well as mutual overlaps. Backgrounds on each side of the measured peaks were chosen away from peaks of the other elements. The intensities of the $K\alpha$ lines of Al and Si, of the $L\alpha$ lines of Y and Zr, and of the $M\alpha$ line of Hf were measured using a TAP crystal. Intensities of the $K\alpha$ lines of P and Ca, of the $L\alpha$

**TABLE 1.** Zircon sample descriptions

| Sample | Locality/description | Occurrence/ paragenesis | Color | Inclusions | Structural state | Donor/source |
|---|---|---|---|---|---|---|
| 274 | Reinbolt Hills near Amery Ice Shelf, Antarctica (EG556) | granulite pegmatite | black | | metamict | Ed Grew |
| 339 | Chantaburi, Thailand | alluvial | pale red | no inclusions | crystalline | Leon T. Silver |
| 340 | Ratnapura, Sri Lanka (Ceylon 6500) | alluvial (granulite peg) | black | | metamict | Leon T. Silver |
| 341 | Chantaburi, Thailand, "RED" | alluvial | red | no inclusions | crystalline | Leon T. Silver |
| 485 | pure synthetic $ZrSiO_4$* | $Li_2MoO_4$-$MoO_3$ flux grown | colorless | no inclusions | crystalline | Armond Chase |
| 576 | Bedford, Westchester, New York, U.S.A. (Harvard 100833) | "cyrtolite" | brown | xl intergrowth | metamict | Karl Francis |
| 1218 | Southeast Asia (CIT 10011)B | | lt. blue | no inclusions | crystalline | |
| 1222-1 | Thailand (sample Siam M21-30) (unheated) | | colorless | no inclusions | crystalline | Grieger's |
| 1222-2 | Thailand (sample Siam M21-30) (heated) | | colorless | no inclusions | crystalline | Greiger's |
| 1223 | Strangway, Northern Territory, Australia (NMNH 117288)** | | colorless | no inclusions | crystalline | U.S. Nat. Mus. Nat. Hist. |
| 1224 | Ampanobe, Flanarantsoa, Madagascar (brown) | coarse syenitic gneiss | brown | hi biref in cracks | partially metamict | Demethius Pohl |
| 1225a | Ampanobe, Flanarantsoa, Madagascar (black) | coarse syenitic gneiss | black | no inclusions | partially metamict | Demethius Pohl |
| 1225b | Ampanobe, Flanarantsoa, Madagascar (black) | coarse syenitic gneiss | clriss tip | no inclusions | partially metamict | Demethius Pohl |
| 1226 | Tanzania | | | | crystalline | Peter Keller |
| 1228-1 | Poças de Caldas, Minas Gerais, Brazil (CIT 4095)† | hydrothermal vug | green | opq in cracks, avoided | partially metamict | Ed Swaboda |
| 1228-2 | Poças de Caldas, Minas Gerais, Brazil (CIT 4095) | hydrothermal vug | green | no inclusions | partially metamict | |
| 1229 | Kimberley, South Africa | kimberlite | colorless | no inclusions | crystalline | Warren Hamilton |
| 1230 | La Panchita, Mexico | | violet | in cracks, avoidable | partially metamict | Leon T. Silver |
| 1231 | Golding Keene, Ontario, Canada (no. 108) | nepheline syenite peg | straw | no inclusions | partially metamict | Leon T. Silver |
| 1232 | Wilberforce, Ontario, Canada | | pale brown | biref in cracks | partially metamict | Leon T. Silver |
| 1233 | Southeast Asia (CIT 10011)A | | colorless | no inclusions | crystalline | |
| 1238 | Ratnapura, Sri Lanka (Ceylon gem 1-24) | alluvial (granulite peg) | green | no inclusions | metamict | Leon T. Silver |
| 1465 | Sigalani Village, Tambani area, Blantyre, Malawi | alluvial | tan-brown | numerous xl and fluid | metamict | Minerals Unlimited |
| 1466 | Fredericksberg, Norway | nepheline syenite peg | dark brown | numerous dusty opq | nearly metamict | purchased |
| 1467-1 | Henderson Co., North Carolina, U.S.A. | alluvial | tan | numerous cracks/incl | nearly metamict | purchased |
| 1467-2 | Henderson Co., North Carolina, U.S.A. | alluvial | tan | numerous cracks/incl | nearly metamict | purchased |
| 1468-1 | Sonora, Mexico (CIT 7570) | | orange | prismatic inclusions | crystalline | |
| 1468-2 | Sonora, Mexico (CIT 7570) | | light red | prismatic inclusions | crystalline | |
| 1469 | Uralla, New South Wales, Australia | | brown | numerous dusty opq | nearly metamict | purchased |
| 1472 | Sieland, Norway (CIT 13217) | pegmatite | brown | hi biref in cracks | partially metamict | Anthony Jones |
| 1473 | Indiahoma, Oklahoma, U.S.A. (CIT 8506) | | brown | numerous xl and dusty | nearly metamict | R.M. Wilke |

* Chase and Osmer (1966).
** Özkan et al. (1974).
† Franco and Loewenstein (1948).

line of Nb, of the $M\alpha$ line of Th, and the $M\beta$ line of U were measured using a PET crystal. Intensities of the $K\alpha$ lines of Ti, Mn, and Fe were measured using a LiF crystal. Beam sizes of 20–30 $\mu$m were used to avoid damaging the more metamict samples. Probe data were reduced using the program CITZAF1, version 3.03, (Armstrong, 1988) employing the Phi(RhoZ) absorption correction of Armstrong (1982), the fluorescence correction of Reed (1965) as modified by Armstrong (1982), the Love and Scott atomic number correction, the Phi (0) equation, a backscatter correction (Love et al., 1978), and mean ionization potentials of Berger and Seltzer. Analyses of each sample are listed in Table 3; structural formulas normalized to four O atoms are listed in Table 4.

## RESULTS AND DISCUSSION

### Spectroscopic features

The portion of the IR spectra from 4000 to 2500 $cm^{-1}$ of the zircon samples studied is remarkably diverse.

**TABLE 2.** Infrared band intensities for zircon samples

| | Combination modes | | | | OH-stretching modes | | | | | | | | |
|---|---|---|---|---|---|---|---|---|---|---|---|---|---|
| | 2750 | 3200 | 3100 | 32/31 | 3420 | | 3385 | | ∥ : ⊥ | Other OH-stretching bands observed | | | |
| Sample | E∥c | E⊥c | E⊥c | Ratio | E∥c | posn. | E⊥c | posn. | Ratio | band | posn. | band | posn. |
| 274 | 0.000 | 0.000 | 0.000 | — | 2.990 | 3430 | 2.640 | 3450 | 1.13 | | | | |
| 339 | 0.721 | 1.120 | 0.398 | 2.82 | 0.108 | 3419 | 0.036 | 3387 | 3.00 | 0.031 | 3328 | | |
| 340 | 0.000 | 0.000 | 0.000 | — | 6.930 | 3498 | 6.930 | 3498 | 1.00 | | | | |
| 341 | 0.669 | 2.925 | 1.836 | 1.59 | 0.866 | 3420 | 0.164 | 3384 | 5.27 | 0.036 | 3560 | | 3350 |
| 486 | 0.767 | 0.000 | 0.000 | — | 0.000 | — | 0.000 | — | — | | | | |
| 576 | 0.000 | 0.000 | 0.000 | — | 2.381 | 3424 | 2.560 | 3379 | 0.93 | 0.267 | 3618 | 0.124 | 3595 |
| 1218 | 0.810 | 3.408 | 5.070 | 0.67 | 0.001 | 3422 | 0.000 | — | — | | | | |
| 1222-1 | 0.791 | 1.597 | 0.760 | 2.10 | 0.296 | 3417 | 0.095 | 3383 | 3.13 | | | | |
| 1222-2 | 0.765 | 1.523 | 0.902 | 1.69 | 0.280 | 3417 | 0.088 | 3383 | 3.18 | | | | |
| 1223 | 0.772 | 1.506 | 1.060 | 1.42 | 0.000 | — | 0.000 | — | — | 0.022 | 3325 | | |
| 1224 | 0.366 | 0.000 | 0.000 | — | 2.356 | 3410 | 2.089 | 3377 | 1.13 | 1.722 | 3701 | 0.124 | 3664 |
| 1225a | 0.000 | 0.000 | 0.000 | — | 6.906 | 3436 | 5.874 | 3386 | 1.18 | | | | |
| 1255b | 0.000 | 0.000 | 0.000 | — | 6.278 | 3430 | 5.112 | 3380 | 1.23 | | | | |
| 1226 | 0.679 | 0.000 | 0.000 | — | 0.452 | 3390 | 0.050 | 3350 | — | 0.924 | 3280 | | |
| 1228-1 | 0.357 | 0.000 | 0.000 | — | 12.143 | 3420 | 4.167 | 3385 | 2.91 | 0.167 | 3563 | 1.333 | 3510 |
| 1228-2 | 0.363 | 0.000 | 0.000 | — | 17.976 | 3418 | 8.690 | 3386 | 2.07 | 0.286 | 3563 | 0.690 | 3510 |
| 1229 | 0.741 | 0.424 | 0.200 | 2.12 | 2.012 | 3417 | 0.859 | 3384 | 2.34 | 0.099 | 3510 | | |
| 1230 | 0.359 | 0.071 | 0.089 | 0.80 | 3.089 | 3395 | 0.893 | 3385 | 3.46 | 4.171 | 3275 | | |
| 1231 | 0.159 | 0.000 | 0.000 | — | 3.723 | 3432 | 3.069 | 3370 | 1.21 | | | | |
| 1232 | 0.409 | 0.000 | 0.000 | — | 0.727 | 3390 | 0.864 | 3290 | 0.84 | | | | |
| 1233 | 0.818 | 1.353 | 0.776 | — | 0.000 | — | 0.000 | — | — | | | | |
| 1238 | 0.000 | 0.000 | 0.000 | — | 1.080 | | 1.080 | | 1.00 | | | | |
| 1465 | 0.000 | 0.000 | 0.000 | — | 21.188 | 3358 | 21.749 | 3334 | 0.97 | 0.573 | 3695 | 0.358 | 3621 |
| 1466 | 0.235 | 0.000 | 0.000 | — | 18.358 | 3402 | 15.299 | 3340 | 1.20 | 1.000 | 3697 | 0.418 | 3622 |
| 1467-1 | 0.146 | 0.000 | 0.000 | — | 9.281 | 3380 | 8.922 | 3325 | 1.04 | 2.748 | 3700 | 2.162 | 3625 |
| 1467-2 | 0.000 | 0.000 | 0.000 | — | 11.078 | 3480 | 10.240 | 3430 | 1.08 | 8.065 | 3696 | 4.922 | 3621 |
| 1468-1 | 0.620 | 7.843 | 8.690 | 0.90 | 0.161 | 3425 | 0.000 | — | — | 0.200 | 3890 | 0.132 | 3825 |
| 1468-2 | 0.761 | 2.404 | 4.247 | 0.57 | 0.101 | 3421 | 0.022 | 3384 | 4.50 | | | | |
| 1469 | 0.058 | 0.000 | 0.000 | — | 20.424 | 3413 | 17.857 | 3340 | 1.14 | 0.246 | 3701 | | |
| 1472 | 0.519 | 0.000 | 0.000 | — | 0.746 | 3420 | 0.269 | 3385 | 2.78 | 4.819 | 3539 | 2.922 | 3323 |
| 1473 | 0.000 | 0.000 | 0.000 | — | 11.839 | 3400 | 9.283 | 3350 | 1.28 | | | | |

Spectra of metamict zircon (Fig. 1), crystalline zircon (Fig. 2), and partially metamict zircon (Fig. 3) show a wide range of OH-stretching features and a strong effect of radiation damage on their appearance. Woodhead et al. (1991) showed that the strength of the combination-mode triplet at ~2750 $cm^{-1}$ in the $\mathbf{E} \perp \mathbf{c}$ polarization is a measure of crystallinity in the Sri Lanka zircon suite. That band is weak or absent in the zircon spectra shown in Figure 1. These samples are thus metamict or nearly so. Their IR spectra are representative of those of all the highly radiation-damaged samples listed in Table 1. The isotropic, or nearly isotropic, bands with peaks between 3300 and 3500 $cm^{-1}$ (Table 2) result from the stretching mode of OH. Although their broad, asymmetric shapes are reminiscent of bands resulting from unoriented $H_2O$ in some other silicates, no structural $H_2O$ has been detected. $H_2O$ can be distinguished from OH on IR spectra by the presence of the H-O-H bending mode at ~1600 $cm^{-1}$ and the H-O-H combination mode at ~5200 $cm^{-1}$. The absence of those bands from the spectra of inclusion-free zircon indicates that $H_2O$ is below detectability. In the inclusion-free samples with relatively strong OH-stretching mode bands, the OH overtone mode at ~6665 $cm^{-1}$ is readily seen, but the H-O-H combination mode at ~5200 $cm^{-1}$, which is equally intense in $H_2O$, is not present. This confirms that OH is the only hydrous species present in those samples.

The breadth of the OH-stretching band in the spectra of metamict zircon is a result of the multitude of OH environments caused by the structural disorder brought about by radiation damage during the metamictization process. Several samples have a maximum intensity of the OH-stretching band of about three times that of Sri Lanka zircon 6500 (no. 340), the most OH-rich sample found in our previous study (Woodhead et al., 1991). Beer's law calculations suggest that the maximum OH content in our samples is about 0.1 wt% expressed as $H_2O$. These calculations are based on molar absorptivity data for the broad OH-stretching band in glass (Newman et al., 1986; $\epsilon = 100$) because no calibration of the relationship between IR band strength and OH content in zircon is yet available.

Some additional sharp OH-stretching bands that occur at ~3700 and ~3625 $cm^{-1}$ are quite strong in the IR spectra of a few zircon samples and are detectable in others (Table 2). Weaker bands at ~3660 and ~3560 $cm^{-1}$ associated with the other two sometimes also can be discerned. These bands are invariably isotropic, even in partially metamict samples with anisotropic OH-stretching bands at ~3400 $cm^{-1}$. They occur only in samples that contain numerous distributed dusty inclusions or numerous cracks filled with inclusions (Table 1). In a search of IR spectra of minerals, we found that the only matches for these bands are in the spectrum of kaolinite, which matched perfectly, or in the spectra of two other kaolinite-group minerals, halloysite and dickite, which matched

**TABLE 2**—*Continued*

| OH-stretching modes | | | | | |
|---|---|---|---|---|---|
| | | Other OH-stretching bands observed | | | |
| band | posn. | band | posn. | band | posn. |
| 0.036 | 3292 | | | | |
| 0.476 | 3379 | 0.086 | 3310 | | |
| 1.611 | 3624 | 0.058 | 3554 | | |
| 20.476 | 3264 | | | | |
| 18.952 | 3261 | | | | |
| 0.022 | 3600 | | | | |
| 0.143 | 3560 | | | | |
| 0.418 | 3555 | | | | |
| 0.108 | 3470 | 0.301 | 3229 | 0.500 | 3180 |

**TABLE 4.** Zircon formulas based on electron microprobe analyses

| Sample | Formulas |
|---|---|
| 274 | $Zr_{0.964}Hf_{0.032}Mn_{0.001}U_{0.004}Si_{0.996}P_{0.002}Al_{0.001}O_4$ |
| 339 | $Zr_{0.986}Hf_{0.013}Ti_{0.001}Fe_{0.001}Si_{1.000}O_4$ |
| 340 | $Zr_{0.935}Hf_{0.055}Y_{0.003}Th_{0.001}U_{0.006}Si_{0.991}P_{0.002}O_4$ |
| 341 | $Zr_{1.000}Hf_{0.020}Si_{0.980}O_4$ |
| 485 | $Zr_{0.998}Si_{1.001}O_4$ |
| 576a | $Zr_{0.971}Hf_{0.024}Ca_{0.004}Mn_{0.001}Fe_{0.006}Y_{0.003}Th_{0.001}U_{0.003}Si_{0.990}P_{0.003}O_4$ |
| 1218 | $Zr_{1.008}Hf_{0.011}Si_{0.981}O_4$ |
| 1222-1 | $Zr_{0.991}Hf_{0.012}Ca_{0.001}Si_{0.996}O_4$ |
| 1222-2 | $Zr_{0.990}Hf_{0.011}Ca_{0.001}Si_{0.998}O_4$ |
| 1223 | $Zr_{0.989}Hf_{0.020}Si_{0.990}O_4$ |
| 1224 | $Zr_{0.986}Hf_{0.016}Si_{0.997}O_4$ |
| 1225a | $Zr_{0.979}Hf_{0.021}Ti_{0.001}Mn_{0.001}Si_{0.997}O_4$ |
| 1225b | $Zr_{0.978}Hf_{0.021}Ti_{0.001}Si_{0.997}O_4$ |
| 1228-1 | $Zr_{0.982}Hf_{0.009}Ca_{0.002}Mn_{0.002}Fe_{0.004}Si_{1.004}O_4$ |
| 1228-2 | $Zr_{0.994}Hf_{0.010}Ca_{0.003}Mn_{0.003}Fe_{0.002}Si_{0.992}O_4$ |
| 1229 | $Zr_{0.985}Hf_{0.016}Si_{0.999}O_4$ |
| 1230 | $Zr_{0.991}Hf_{0.011}Ti_{0.001}Si_{0.997}O_4$ |
| 1231 | $Zr_{0.993}Hf_{0.008}U_{0.001}Si_{0.997}O_4$ |
| 1232 | $Zr_{0.990}Hf_{0.011}Si_{0.999}O_4$ |
| 1233 | $Zr_{0.998}Hf_{0.011}Ti_{0.001}Si_{0.990}O_4$ |
| 1238 | $Zr_{0.936}Hf_{0.058}U_{0.006}Si_{0.983}O_4$ |
| 1465 | $Zr_{0.987}Hf_{0.013}Fe_{0.001}Y_{0.002}U_{0.001}Si_{0.995}Al_{0.003}O_4$ |
| 1466a | $Zr_{0.978}Hf_{0.018}Fe_{0.005}Y_{0.003}Th_{0.003}U_{0.002}Si_{0.994}Al_{0.001}O_4$ |
| 1466b* | $Th_{0.805}U_{0.056}Zr_{0.042}Ca_{0.009}Ti_{0.002}Fe_{0.014}Y_{0.024}Si_{0.592}Al_{0.096}O_4$ |
| 1467-1 | $Zr_{0.982}Hf_{0.014}Y_{0.001}Th_{0.002}U_{0.001}Si_{1.001}O_4$ |
| 1468-1 | $Zr_{0.984}Hf_{0.010}Fe_{0.001}Y_{0.007}U_{0.001}Si_{0.998}O_4$ |
| 1468-2 | $Zr_{0.988}Hf_{0.010}Y_{0.002}U_{0.001}Si_{0.999}O_4$ |
| 1469 | $Zr_{0.974}Hf_{0.011}Ca_{0.001}Ti_{0.001}Fe_{0.001}Y_{0.004}Th_{0.003}U_{0.001}Si_{1.005}Al_{0.002}O_4$ |
| 1472 | $Zr_{0.990}Hf_{0.010}Si_{0.999}Al_{0.001}O_4$ |
| 1473 | $Zr_{0.966}Hf_{0.030}Y_{0.005}U_{0.001}Si_{0.990}P_{0.006}O_4$ |

* Thorite inclusion in zircon from Fredericksberg, Norway.

**TABLE 3.** Electron microprobe analyses of zircon samples

| Sample | $Al_2O_3$ | $SiO_2$ | CaO | $TiO_2$ | MnO | FeO | $P_2O_5$ | $ZrO_2$ | $Y_2O_3$ | $HfO_2$ | $ThO_2$ | $UO_2$ | Total* |
|---|---|---|---|---|---|---|---|---|---|---|---|---|---|
| 274 | 0.03(3)** | 32.47(6) | —† | — | 0.03(2) | — | 0.08(1) | 64.46(13) | — | 3.64(3) | — | 0.52(5) | 101.25 |
| 339 | — | 32.76(7) | — | 0.05(2) | — | 0.03(1) | — | 66.24(13) | — | 1.44(2) | — | — | 100.56 |
| 340 | — | 31.68(6) | — | — | — | — | 0.07(1) | 61.36(13) | 0.21(1) | 6.12(4) | 0.09(3) | 0.83(5) | 100.98 |
| 341 | — | 31.19(6) | — | — | — | — | — | 65.25(13) | — | 2.23(3) | 0.06(3) | — | 98.76 |
| 485 | — | 32.64(7) | — | — | — | — | — | 66.74(13) | — | — | — | — | 99.41 |
| 576a | — | 31.46(6) | 0.12(1) | — | 0.05(2) | 0.23(1) | 0.09(1) | 63.22(13) | 0.19(1) | 2.64(3) | 0.15(3) | 0.42(5) | 98.57 |
| 1218 | — | 31.08(6) | — | — | — | — | — | 65.50(13) | — | 1.19(2) | — | — | 97.80 |
| 1222-1 | — | 32.53(6) | 0.02(1) | — | — | — | — | 66.33(13) | — | 1.40(2) | — | — | 100.32 |
| 1222-2 | — | 32.43(7) | 0.02(1) | — | — | — | — | 65.97(13) | — | 1.24(2) | — | — | 99.68 |
| 1223 | — | 31.84(6) | — | — | — | 0.02(1) | — | 65.22(13) | — | 2.29(3) | — | — | 99.39 |
| 1224 | — | 32.69(7) | 0.01(1) | — | — | — | — | 66.34(13) | — | 1.85(3) | 0.05(3) | — | 100.98 |
| 1225a | — | 32.20(6) | — | 0.04(2) | 0.03(2) | — | — | 64.96(13) | — | 2.39(3) | — | 0.35(5) | 99.96 |
| 1225b | — | 32.27(6) | — | 0.04(3) | — | — | — | 64.88(13) | — | 2.41(3) | — | 0.40(5) | 100.03 |
| 1228-1 | — | 32.57(7) | 0.05(1) | — | 0.09(1) | 0.16(3) | — | 65.33(13) | — | 1.02(2) | — | 0.05(4) | 99.30 |
| 1228-2 | — | 31.99(6) | 0.09(1) | — | 0.13(2) | 0.06(1) | — | 65.73(13) | — | 1.12(2) | — | — | 99.17 |
| 1229 | — | 32.50(7) | — | — | — | — | — | 65.72(13) | — | 1.81(3) | — | — | 100.05 |
| 1230 | — | 32.57(7) | — | 0.04(2) | — | — | — | 66.36(13) | — | 1.26(2) | — | — | 100.29 |
| 1231 | — | 32.28(6) | — | — | — | — | — | 65.91(13) | — | 0.92(2) | — | 0.14(4) | 99.28 |
| 1232 | — | 32.35(6) | — | — | — | — | — | 65.71(13) | — | 1.21(2) | — | — | 99.29 |
| 1233 | — | 31.89(6) | — | 0.06(2) | — | — | — | 65.93(13) | — | 1.19(2) | — | — | 99.08 |
| 1238 | — | 31.17(6) | — | — | — | 0.04(1) | — | 60.87(13) | — | 6.50(4) | 0.03(3) | 0.81(5) | 100.82 |
| 1465 | 0.07(1) | 31.89(6) | — | — | — | 0.02(1) | — | 64.85(13) | 0.12(1) | 1.46(2) | — | 0.10(4) | 98.57 |
| 1466a | 0.04(1) | 31.96(6) | — | — | — | 0.18(1) | — | 64.44(13) | 0.19(1) | 1.99(3) | 0.38(4) | 0.25(4) | 99.43 |
| 1466b‡ | 1.40(1) | 10.22(4) | 0.15(1) | 0.05(3) | — | 0.29(2) | 6.51(5) | 1.50(03) | 0.77(2) | — | 61.01(24) | 4.37(9) | 86.30 |
| 1467-1 | — | 32.04(6) | 0.01(1) | — | — | 0.01(1) | — | 64.42(13) | 0.04(1) | 1.55(2) | 0.22(3) | 0.10(4) | 98.39 |
| 1468-1 | — | 32.16(6) | — | — | — | 0.05(1) | — | 65.07(13) | 0.43(2) | 1.14(2) | 0.04(3) | 0.09(4) | 99.01 |
| 1468-2 | — | 32.35(6) | — | — | — | 0.02(1) | — | 65.62(13) | 0.13(1) | 1.18(2) | — | 0.11(4) | 99.44 |
| 1469 | 0.06(1) | 32.49(6) | 0.03(1) | 0.04(2) | — | 0.03(1) | — | 64.60(13) | 0.24(1) | 1.24(2) | 0.38(4) | 0.10(4) | 99.22 |
| 1472 | 0.03(1) | 32.59(7) | — | — | — | — | — | 66.22(13) | — | 1.09(2) | — | — | 99.93 |
| 1473 | — | 31.86(6) | — | — | — | 0.02(1) | 0.24(2) | 63.75(13) | 0.29(1) | 3.37(3) | — | 0.21(4) | 99.73 |

* Nb analyzed for in all samples, but not present.
** Units in parentheses represent one standard deviation counting error on least units cited.
† Dash: not detected or counting statistics error >75%.
‡ Thorite inclusion in zircon from Fredericksberg, Norway.

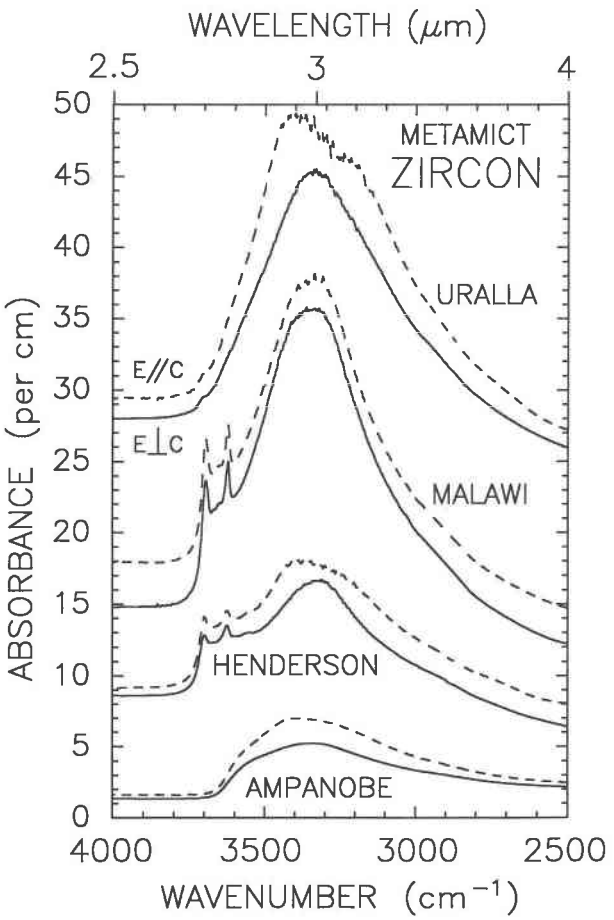


Fig. 1. Polarized infrared spectra of four samples of metamict zircon: Uralla, New South Wales, Australia (no. 1469); Sigwani Village, Malawi (no. 1465); Henderson, North Carolina (no. 1467); and Ampanobe (black), Madagascar (no. 1225). In this and the following figures spectra have been vertically offset for clarity.

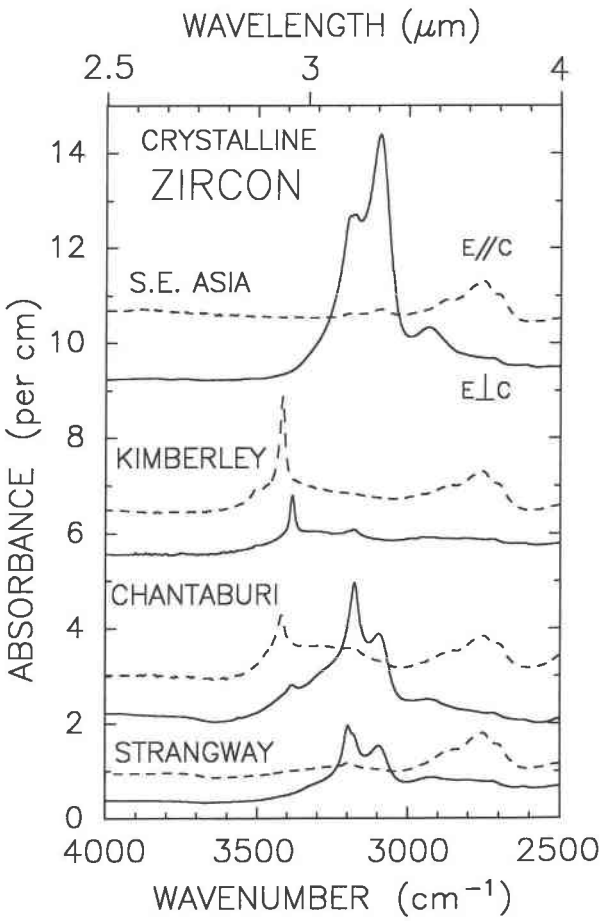


Fig. 2. Polarized infrared spectra of four samples of crystalline zircon: southeast Asia (no. 1218); Kimberley (no. 1229); Chantaburi, Thailand (no. 341); and Strangway, Northern Territory, Australia (no. 1223).

less well. The sharp bands in the 3550–3700 $cm^{-1}$ range thus are not related to hydrous species directly incorporated into the zircon structure.

The Uralla and Malawi samples both contain numerous fluid inclusions. The presence of the H-O-H bending-mode overtone at 5185 $cm^{-1}$ in their IR spectra confirms that $H_2O$ is present in the fluid inclusions. The combination of $H_2O$ in fluid inclusions and OH in kaolinite inclusions probably accounts for at least two-thirds of the OH present in these two samples. Thus, even the estimate of 0.1 wt% is probably too high by a factor of 3.

The IR spectra of crystalline zircon (Fig. 2) bear little resemblance to those of metamict zircon. In the representative spectra shown, the combination-mode band at ~2750 $cm^{-1}$ ($\mathbf{E} \| \mathbf{c}$) has an intensity of at least 0.6 per cm, indicating a lack of radiation damage. Other bands in the spectra at ~3510 $cm^{-1}$ ($\mathbf{E} \| \mathbf{c} > \mathbf{E} \perp \mathbf{c}$), ~3420 $cm^{-1}$ ($\mathbf{E} \| \mathbf{c}$), ~3385 $cm^{-1}$ ($\mathbf{E} \perp \mathbf{c}$), ~3200 $cm^{-1}$ ($\mathbf{E} \perp \mathbf{c}$), ~3180 $cm^{-1}$ ($\mathbf{E} \perp \mathbf{c}$), and ~3100 $cm^{-1}$ ($\mathbf{E} \perp \mathbf{c}$) exhibit considerable variability. The pair of sharp bands at ~3420 $cm^{-1}$ ($\mathbf{E} \| \mathbf{c}$) and ~3385 $cm^{-1}$ ($\mathbf{E} \perp \mathbf{c}$) are OH bands resulting from trace amounts of oriented OH. They indicate the presence of a hydrous component in several of the natural crystalline zircon samples. Their absence in the spectra of other samples shows them to be anhydrous.

The Kimberley zircon exhibits the strongest OH-stretching mode band of any crystalline zircon studied. Because the Beer's law calculation used above for the metamict samples cannot be applied to the sharp bands in crystalline zircon spectra, another means of estimating OH content is needed. Robinson et al. (1971) showed that the crystal structure of zircon is similar to that of garnet in many ways. Rossman and Aines (1991) calibrated IR spectra and OH content in grossular. Using their integrated absorbance calibration factor (3746 per mol/L OH per cm) as an approximation for crystalline zircon yields an OH content of 0.007 wt%, expressed as $H_2O$.

The weak, sharp absorption bands at 3510 $cm^{-1}$ ($\mathbf{E} \| \mathbf{c}$) and 3504 $cm^{-1}$ ($\mathbf{E} \perp \mathbf{c}$) in the IR spectrum of the Kimberley zircon (Table 2) are at essentially the same position

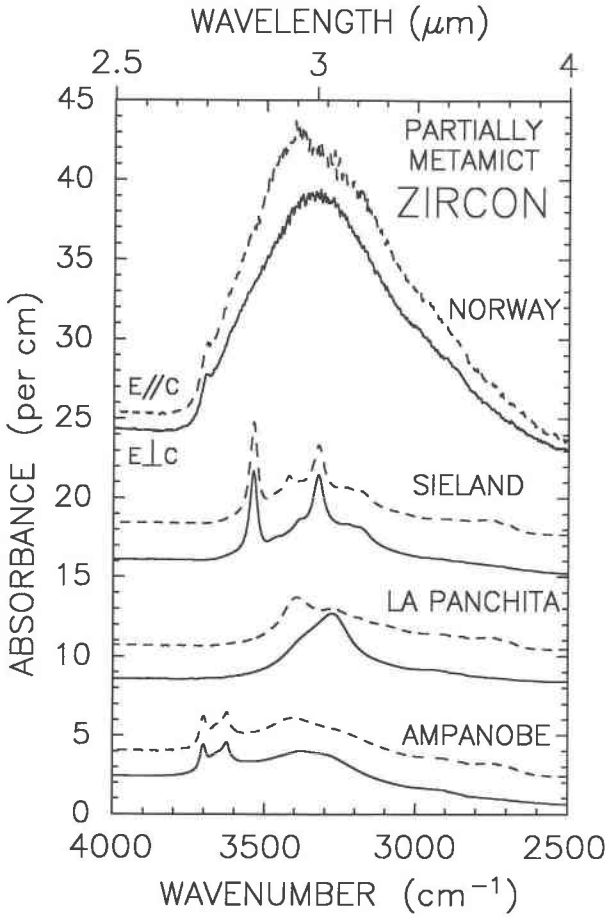


Fig. 3. Polarized infrared spectra of four samples of partially metamict zircon: Fredericksberg, Norway (no. 1466); Sieland pegmatite, Norway (no. 1472); La Panchita pegmatite, Mexico (no. 1230); Ampanobe (brown), Madagascar (no. 1224).

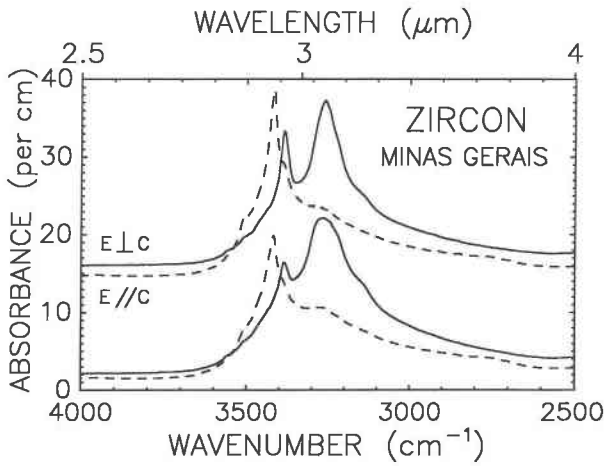


Fig. 4. Polarized infrared spectra of two samples of partially metamict zircon from Poças de Caldas, Minas Gerais, Brazil (1228-1 and 1228-2).

as the OH-stretching band detected by Caruba et al. (1985) in their unpolarized IR spectra of synthetic hydroxylated zircon. Those bands are considerably less intense than the prominent OH bands at 3417 $cm^{-1}$ (**E**∥**c**) and 3384 $cm^{-1}$ (**E**⊥**c**), however. If this is in fact the same band as reported by Caruba et al., then the hydrogrossular substitution $[4(OH)^-] \leftrightarrow [(SiO_4)^{4-}]$ does occur in natural crystalline zircon, but is not the most important OH site.

The highly variable bands at ~3200, ~3180, and ~3100 $cm^{-1}$ are in an unusually low-energy range for OH-stretching modes and are more likely to be the result of lattice vibration combination modes. However, the tail of the broad OH band in the metamict zircon extends to even lower wavenumbers, and OH bands with similarly low energies are known to occur in other orthosilicates such as sillimanite (3248 $cm^{-1}$; Beran et al., 1989) and phenakite (3120 $cm^{-1}$; Beran, 1990). It is thus possible that the bands result from the presence of OH in an orientation where the O-H···O bond distance is unusually short. We conducted the crystalline zircon heating experiment discussed below to determine the identity of these bands.

The IR spectra of partially metamict zircon (Fig. 3) are characterized by weak combination-mode bands at ~2750 (**E**⊥**c**) and exhibit features intermediate between the spectra of metamict and crystalline zircon. The zircon samples shown have a wide range of crystallinities. Their IR spectra are noticeably anisotropic in the OH-stretching region. The OH band at about 3400 $cm^{-1}$ is much like similar bands in metamict zircon, but its breadth depends on the degree of metamictization of the sample. Its position and strength depend on the polarization of the incident IR beam. This indicates a tendency for the OH to be crystallographically aligned in the partially radiation-damaged structure. The maximum OH content is again calculated to be approximately 0.1 wt%.

Sharp, isotropic kaolinite bands can be seen in the spectrum from Ampanobe (brown) (no. 1224) and probably result from the myriad of dusty, birefringent inclusions in numerous cracks [in contrast to the cleaner, but more radiation-damaged, Ampanobe sample (black) (no. 1225) specimen of Fig. 1]. The La Panchita zircon sample exhibits a strong band at 3275 $cm^{-1}$ (**E**⊥**c**), and some indication of the same band can be seen in the Ampanobe (brown) zircon spectrum. As both samples contain numerous inclusions in cracks, these bands cannot be assigned unambiguously to structural OH in zircon without further confirmation. The slightly radiation-damaged Sieland pegmatite zircon has a particularly complex spectrum. The weak, relatively sharp anisotropic bands at 3420 $cm^{-1}$ (**E**∥**c**) and 3385 $cm^{-1}$ (**E**⊥**c**) are the same OH bands observed in OH-bearing nonmetamict zircon. The isotropic bands at 3539, 3470, 3323, 3230, and 3180 $cm^{-1}$ are probably the result of inclusions in the numerous cracks in the specimen.

The zircon samples from Minas Gerais, Brazil, (no. 1228) (Fig. 4) are partially metamict grains from within

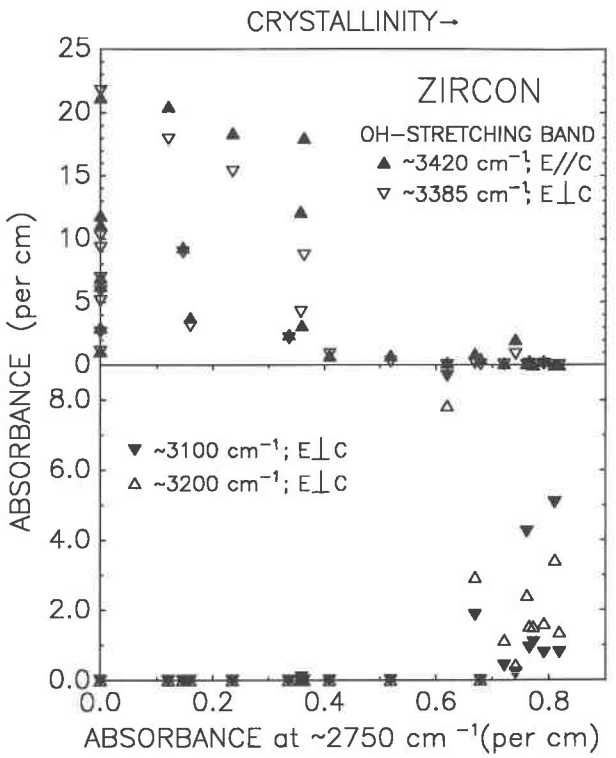


Fig. 5. Plots of infrared band intensities as functions of crystallinity for the zircon samples studied (Table 2): **(top)** OH-stretching band intensities in two polarizations vs. intensity at ~2750 cm$^{-1}$ (**E**‖**c**). **(bottom)** IR band intensities at ~3100 and ~3200 cm$^{-1}$ (**E**⊥**c**) vs. intensity at ~2750 cm$^{-1}$ (**E**‖**c**).

a few centimeters of each other in a single hydrothermal vug (Franco and Loewenstein, 1948). Hydrothermal zircon is not common, but one might expect it to be enriched in OH if zircon really can take up OH during growth. The OH-stretching bands at 3420 cm$^{-1}$ (**E**‖**c**) and 3385 cm$^{-1}$ (**E**⊥**c**) are sharp and among the strongest observed in all the samples studied. They probably represent primary OH incorporated during the crystallization of the zircon in an environment with high $H_2O$ activity. The high OH content may be zoned or only metastable, however, as these two samples of identical paragenesis exhibit band strengths that differ by approximately 50% (Fig. 4). The OH content of the grain with the most OH is about 0.05 wt% (as $H_2O$) based on the grossular calibration of Rossman and Aines (1991), modified to account for the lower wavenumber of the zircon OH absorption band using the intensity vs. wavenumber correlation of Paterson (1982).

The strong bands at 3263 cm$^{-1}$ (**E**⊥**c** > **E**‖**c**) also differ in both strength and breadth among spectra for grains. Because the Minas Gerais zircon samples are virtually free of inclusions, the band at 3263 cm$^{-1}$ probably results from an additional OH orientation. The band's similarity in position and polarization to the unassigned bands in the La Panchita and Ampanobe (brown) zircon spectra suggests that they, too, are genuine zircon hydroxyl bands in partially metamict samples.

The sharp bands at 3508 (**E**‖**c**) and 3510 cm$^{-1}$ (**E**⊥**c**) in the Minas Gerais spectra coincide with the OH band of Caruba's hydroxylated zircon (Caruba et al., 1985). They are an order of magnitude stronger than in the Kimberley zircon, but the hydrogrossular substitution [4(OH)$^-$] ↔ [$(SiO_4)^{4-}$] is still not the dominant OH site.

The systematic relationship between OH and degree of metamictization is of particular interest in zircon. A plot of band strengths at ~3420 cm$^{-1}$ (**E**‖**c**) and ~3385 cm$^{-1}$ (**E**⊥**c**) vs. ~2750 cm$^{-1}$ (Fig. 5) shows relative OH content as a function of crystallinity. The zircon spectra fall approximately into three crystallinity groups: crystalline, with ~2750 cm$^{-1}$ intensities greater than 0.6; metamict, with intensities of zero; and partially metamict, with intermediate intensities. Although OH-stretching bands are evident in the IR-absorption patterns of several of the crystalline zircon samples, their OH contents are apparently restricted to very low values. The crystalline zircon with the highest OH content is the Kimberley sample (no. 1229), a mantle-derived zircon sample from a kimberlite pipe. This suggests a considerably higher activity of OH in zircon-forming environments in the mantle than in the majority of such crustal environments, consistent with results from other minerals such as olivine (Miller et al., 1987) and pyroxene (Skogby et al., 1990). We have little information about the parageneses of the rest of the crystalline zircon samples.

The OH contents of the metamict and partially metamict samples exhibit about an order of magnitude more variability than the crystalline samples. Some are nearly as anhydrous as their crystalline analogues, while others contain much more OH. This pattern contrasts with the situation in the Sri Lanka zircon suite (Woodhead et al., 1991), in which only totally metamict samples exhibited OH-stretching bands of greater than 1 absorbance unit per cm. If the structural OH in radiation-damaged zircon represents a primary hydrous species, there should be a correlation between the amount of OH detected and the expected activity of $H_2O$ in their growth environments. However, pegmatitic zircon samples have OH amounts that span the entire range of the OH contents we observed. Similarly, if alluvial metamict zircon took up secondary OH readily during transport, their OH contents should be higher than other samples. However, the highest and lowest OH content samples are both alluvial. Such variability prevents us from establishing clear correlations between OH content and postcrystallization history. We do note that none of the partially metamict zircon samples in this survey are as anhydrous as those in the Sri Lanka suite.

The bands at ~3200 cm$^{-1}$ (**E**⊥**c**) and ~3100 cm$^{-1}$ (**E**⊥**c**) are absent in metamict and partially metamict zircon, whether high or low in OH content (Fig. 5). They are present only in crystalline zircon but with variable intensities. These data suggest that the bands are not OH-

stretching bands, but may be some extremely sensitive measure of zircon crystallinity.

### Chemical analyses

Electron microprobe analyses (Tables 3 and 4) yielded nearly stoichiometric formulas for all the crystalline zircon samples. Within the error of the analyses, other compounds such as $ZrO_2$ or $SiO_2$ are not intermixed with the zircon. In most of the crystalline samples, the only significant substituent for Zr is Hf. The Sonora zircon contains considerable Y and about 1000 ppm U. Its crystallinity suggests that it is relatively young or has been annealed. There is no relation between Hf content and ~2750 $cm^{-1}$ band strength in the crystalline samples, confirming that the intensity of that band is a valid measure of crystallinity in other suites as well as that from Sri Lanka and not a function of composition. There is no unambiguous correlation between Hf content and band strength at ~3200 and ~3100 $cm^{-1}$ either. Although the natural samples with the lowest Hf contents (nos. 1218 and 1468) exhibited the strongest bands, the pure synthetic zircon (no. 485), with no Hf, exhibited no signs of them at all.

If the OH content of crystalline zircon results from the hydrogrossular substitution $[4(OH)^-] \leftrightarrow [(SiO_4)^{4-}]$, there should be a Si deficiency in the microprobe analyses that matches the OH content inferred from the IR spectra. However, the calculated OH content of the crystalline samples is far below the standard deviation of Si content based on counting statistics, so no OH-Si deficiency correlation could be established.

If the OH content of crystalline zircon results from a charge-balance substitution of the form $[M^{3+} + H^+] \leftrightarrow [Zr^{4+}]$, there should be a net deficit of charge in the structural formulas that matches their OH contents. Taking both Mn and Fe to have valencies of +3, the net charge imbalance of the Kimberley zircon from the probe analyses (−0.0006) virtually matches the approximate mole fraction of H present (0.0005). This cannot be considered positive evidence that the charge-balance substitution takes place, however, because analyses of most of the rest of the crystalline zircon samples indicate similar or greater apparent charge deficiencies even though they contain considerably less OH.

Electron microprobe analyses of metamict and partially metamict samples also yielded nearly stoichiometric structural formulas. A number of samples contain several cations substituting for Zr. Some contain P substituting for Si. The Minas Gerais zircon samples have an unusually high Mn content as well as considerable Fe. Their net charge imbalance (−0.01) is twice the fraction of H present (0.005) in the more hydrated sample and about three times that of the other. These data do not necessarily contradict the $[M^{3+} + H^+] \leftrightarrow [Zr^{4+}]$ substitution scheme; the analyses are simply not precise enough to solve the problem. The Fredericksberg, Norway, sample hosts trace inclusions of euhedral thorite up to a few tens of micrometers across that are easily visualized using backscattered electron imaging. The analysis of the thorite is considerably Si deficient. The Bedford "cyrtolite" is an intergrowth of zircon, quartz, and monazite. The monazite appears to be zoned and recrystallized as viewed in backscattered electron images.

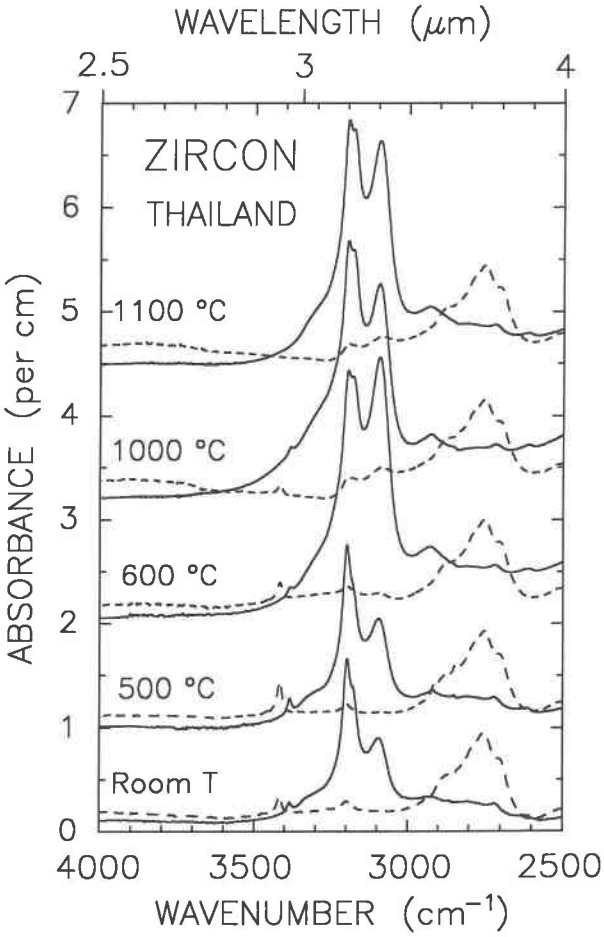


Fig. 6. Selected polarized infrared spectra obtained at room temperature of a crystalline zircon from Thailand (Siam M21-30, no. 1222) subjected to 1-h heating periods at 100 °C intervals from 500 to 1100 °C.

### Heating experiments

To verify that the bands at ~3200 and ~3100 $cm^{-1}$ are not OH bands, we performed a stepwise heating experiment on a crystalline zircon sample (Thailand, no. 1222-2) exhibiting a strong combination-mode band at 2752 $cm^{-1}$ ($\mathbf{E} \| \mathbf{c}$); small, sharp, OH-stretching mode bands at 3417 $cm^{-1}$ ($\mathbf{E} \| \mathbf{c}$) and 3383 $cm^{-1}$ ($\mathbf{E} \perp \mathbf{c}$); and the enigmatic bands at 3198, ~3180, and 3096 $cm^{-1}$ ($\mathbf{E} \perp \mathbf{c}$) (Figs. 6 and 7, Table 5).

There was essentially no change in the crystallinity of the sample on annealing as indicated by the nearly constant strength of the combination-mode band at 2752 $cm^{-1}$ (Figs. 6 and 7). The growth of the bands at 3198

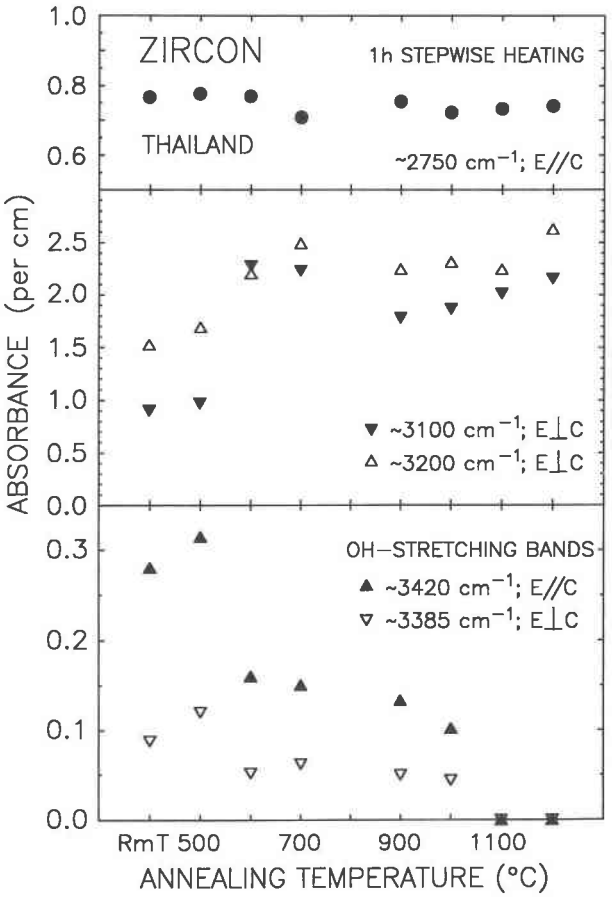


Fig. 7. Plots of infrared band intensities for the Thailand zircon (no. 1222) vs. temperature of annealing: **(top)** IR band intensity at ~2750 $cm^{-1}$ **(E‖c)**. **(middle)** IR band intensities at ~3100 and ~3200 $cm^{-1}$ **(E⊥c)**. **(bottom)** OH-stretching band intensities in two polarizations.

and 3096 $cm^{-1}$ at higher annealing temperatures contrasts sharply with the progressive loss of the anisotropic OH-stretching mode bands at 3417 $cm^{-1}$ (E‖c) and 3383 $cm^{-1}$ (E⊥c), suggesting that the former are not OH bands. The large change in the absolute and relative intensities of the two bands at 600 °C suggests that healing of crystal defects (possibly related to the loss of OH) may be the cause of the effect.

The strengths of the anisotropic OH-stretching bands at 3417 and 3383 $cm^{-1}$ increased during the first annealing at 500 °C and decreased dramatically at 600 °C, the same temperature at which the reorganization of the 3198 and 3096 $cm^{-1}$ bands occurs. They decreased progressively at higher temperatures, becoming undetectable at 1100 °C. The growth of the OH-stretching bands in the first annealing may be the result of the migration of disordered H ions into ordered sites, sharpening and strengthening the OH bands. Subsequent migration of the OH out of the structure results in the loss of the bands at higher temperatures.

To examine the stability of OH in metamict zircon and its relationship with OH in crystalline zircon, we performed a stepwise heating experiment on a nearly metamict zircon sample (Reinbolt Hills, no. 274) (Figs. 8 and 9, Table 6). The sample was oriented for IR study by its external morphology and cut parallel to the (100) face. Although the structure of the highly radiation-damaged zircon was considerably disordered prior to the heating experiment, the polarized IR spectra obtained after high-temperature heating show that the structure recovered its original orientation on annealing. Based on the ~2750 $cm^{-1}$ band, recrystallization did not begin until 1200 °C (Figs. 8 and 9). By 1500 °C the band reached a strength of 0.594 absorbance units per cm, still somewhat less than the 0.7–0.8 values for the same band in the most crystalline samples. The IR spectra in the silicate overtone region of 2100 to 1400 $cm^{-1}$ gave similar results. The spectra remained essentially isotropic (metamict) through the 729 °C heating period. They were anisotropic but broad banded (partially metamict) from 800 to 1100 °C and started to become sharp banded at 1200 °C. A weak band at ~3200 $cm^{-1}$ appeared in the 1400 °C heating period spectrum.

The general shape of the OH-stretching mode band (Figs. 8 and 9) was similar to the unpolarized spectra of the Sri Lanka 6500 metamict zircon sample obtained at temperatures up to 800 °C by Aines and Rossman (1985, 1986). Band intensity decreased progressively up to 419 °C while remaining broad and nearly isotropic. At 532 °C the band started to become more anisotropic and sepa-

**TABLE 5.** Stepwise heating of a crystalline zircon sample from Thailand, GRR 1222

| | Combination modes | | | | OH-stretching modes | | | | |
|---|---|---|---|---|---|---|---|---|---|
| | 2750 | 3200 | 3100 | 32/31 | 3420 | | 3385 | | ‖ : ⊥ |
| *T* (°C) | E‖c | E⊥c | E⊥c | Ratio | E‖c | posn. | E⊥c | posn. | Ratio |
| Rm *T* | 0.765 | 1.523 | 0.902 | 1.69 | 0.280 | 3417 | 0.088 | 3383 | 3.18 |
| 500 | 0.775 | 1.695 | 0.970 | 1.75 | 0.315 | 3416 | 0.120 | 3383 | 2.63 |
| 600 | 0.768 | 2.204 | 2.282 | 0.97 | 0.160 | 3416 | 0.052 | 3382 | 3.05 |
| 700 | 0.708 | 2.490 | 2.230 | 1.12 | 0.150 | 3416 | 0.062 | 3382 | 2.42 |
| 800 | 800 °C data lost | | | | | | | | |
| 900 | 0.753 | 2.246 | 1.780 | 1.26 | 0.133 | 3417 | 0.050 | 3381 | 2.65 |
| 1000 | 0.721 | 2.315 | 1.864 | 1.24 | 0.102 | 3417 | 0.044 | 3381 | 2.32 |
| 1100 | 0.732 | 2.244 | 2.012 | 1.12 | 0.000 | — | 0.000 | — | — |
| 1100 (18 h) | 0.740 | 2.625 | 2.154 | 1.22 | 0.000 | — | 0.000 | — | — |

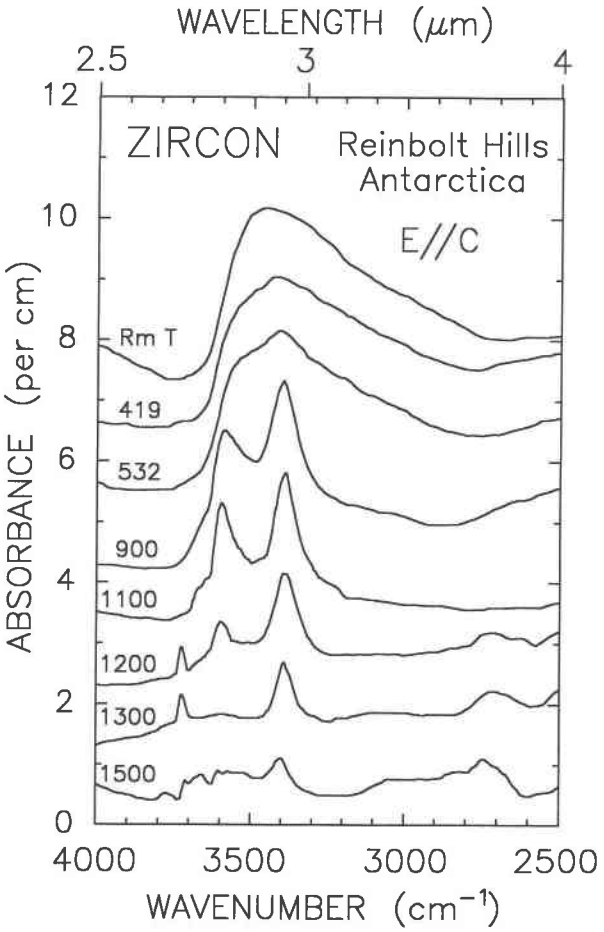


Fig. 8. Selected polarized **E‖c** infrared spectra taken at room temperature of a nearly metamict zircon from Reinbolt Hills, Amery Ice Shelf, Antarctica, (no. 274) subjected to 1-h heating periods at 100 °C intervals from 200 to 1500 °C.

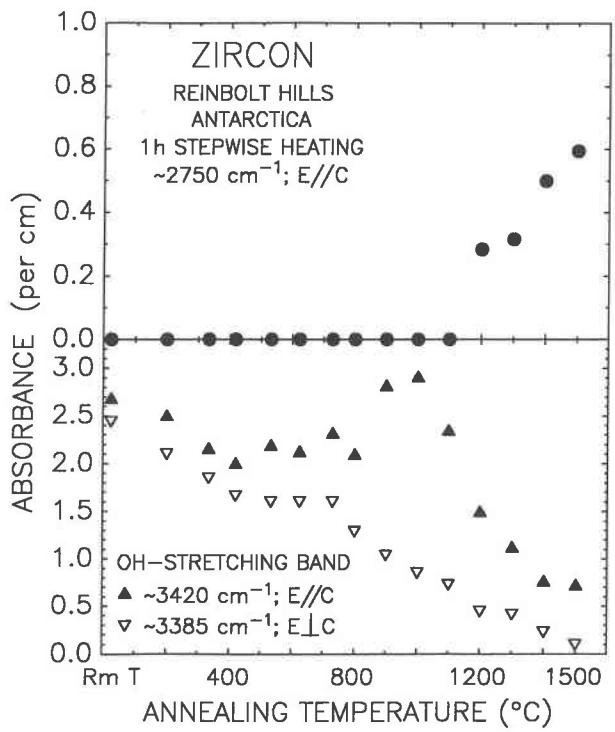


Fig. 9. Plots of infrared band intensities for the Reinbolt Hills, Antarctica, zircon (no. 274) vs. temperature of annealing: **(top)** IR band intensity at ~2750 cm⁻¹ (**E‖c**). **(bottom)** OH-stretching band intensities in two polarizations.

rate into two peaks at ~3400 and ~3600 cm⁻¹. Over the range of 532–1000 °C the strength of both OH peaks in the **E‖c** polarization increased even though their integrated intensities decreased. This probably resulted from the migration of disordered H into ordered sites at the same time much of the OH migrated out of the zircon. A third OH band at ~3725 cm⁻¹ appeared at 1200 °C, increased in intensity at 1300 °C, and then decreased along with the band at ~3600 cm⁻¹. The broad, weak, irregular anisotropic peaks between approximately 3500 and 3800 cm⁻¹ in the 1500 °C spectrum suggest the presence of trace amounts of OH in a number of disordered sites at the highest annealing temperature. Unfortunately the sample was lost before it could be heated further.

The bands near 3400 cm⁻¹ in both polarizations correspond to the dominant OH-stretching mode band observed in several crystalline zircon samples. Neither of the new bands at ~3600 or ~3725 cm⁻¹ definitely corresponds to any structural OH bands observed in crystalline zircon. Although they are close to the positions of the isotropic OH bands resulting from hydrous inclusions, their strong polarization **E‖c** indicates that they represent structurally oriented OH.

### OH sites and orientations

In Si-deficient zircon, H is bonded to O atoms at the vertices of the vacant tetrahedron, using the hydrogrossular substitution $[4(OH)^-] \leftrightarrow [(SiO_4)^{4-}]$. This substitution has been assigned to the band at 3515 cm⁻¹ in the IR spectra of synthetic hydroxylated zircon by Caruba et al. (1985) and appears to correspond to the bands at 3510 cm⁻¹ in the Kimberley and Minas Gerais zircon samples. The energy of this band is significantly lower than those of the OH bands in members of the grossular-hydrogrossular series (Rossman and Aines, 1991), suggesting a significantly shorter length for the O-H···O H bond of zircon.

The structure of anhydrous, crystalline zircon provides only one unique site for each ion, Zr, Si, and O (Robinson et al., 1971). Thus for zircon with no Si deficiency, there is no question of the O site to which the H will bond. The O is at a vertex of a Si-occupied tetrahedron, bonded to one tetrahedrally coordinated Si and two eightfold coordinated cations on the Zr site. It is quite possible that the H is associated with a lower valency substituent for $Zr^{4+}$ by a coupled substitution of the for $[M^{3+} + H^+] \leftrightarrow [Zr^{4+}]$, but the minute fraction of such substitutions necessary to account for the trace OH contents in natural

**TABLE 6.** Stepwise heating of a metamict zircon sample, Reinbolt Hills, Amery Ice Shelf, Antarctica

| | Combination modes | | | | OH-stretching modes | | | | | | | | |
|---|---|---|---|---|---|---|---|---|---|---|---|---|---|
| | 2750 | 3200 | 3100 | 32/31 | 3420 | | 3385 | | ∥ : ⊥ | Other OH-stretching bands | | | |
| *T* (°C) | E∥c | E⊥c | E⊥c | Ratio | E∥c | posn. | E⊥c | posn. | Ratio | E∥c | posn. | E∥c | posn. |
| Rm *T* | 0.000 | 0.000 | 0.000 | — | 2.688 | 3440 | 2.438 | 3440 | 1.10 | | | | |
| 200 | 0.000 | 0.000 | 0.000 | — | 2.500 | 3440 | 2.094 | 3475 | 1.19 | | | | |
| 333 | 0.000 | 0.000 | 0.000 | — | 2.156 | 3430 | 1.844 | 3480 | 1.17 | | | | |
| 419 | 0.000 | 0.000 | 0.000 | — | 2.000 | 3430 | 1.656 | 3440 | 1.21 | | | | |
| 532 | 0.000 | 0.000 | 0.000 | — | 2.188 | 3407 | 1.594 | 3500 | 1.37 | 1.781 | 3560 | | |
| 624 | 0.000 | 0.000 | 0.000 | — | 2.125 | 3408 | 1.594 | 3480 | 1.33 | 1.875 | 3540 | | |
| 729 | 0.000 | 0.000 | 0.000 | — | 2.313 | 3410 | 1.594 | 3510 | 1.45 | 1.750 | 3577 | | |
| 800 | 0.000 | 0.000 | 0.000 | — | 2.094 | 3408 | 1.281 | 3500 | 1.63 | 1.750 | 3560 | | |
| 900 | 0.000 | 0.000 | 0.000 | — | 2.813 | 3399 | 1.031 | 3390 | 2.73 | 2.094 | 3591 | | |
| 1000 | 0.000 | 0.000 | 0.000 | — | 2.906 | 3397 | 0.844 | 3390 | 3.44 | 2.344 | 3598 | | |
| 1100 | 0.000 | 0.000 | 0.000 | — | 2.350 | 3398 | 0.719 | 3390 | 3.27 | 1.969 | 3602 | | |
| 1200 | 0.281 | 0.000 | 0.000 | — | 1.500 | 3398 | 0.438 | 3388 | 3.43 | 0.750 | 3607 | 0.531 | 3732 |
| 1300 | 0.313 | 0.000 | 0.000 | — | 1.119 | 3400 | 0.406 | 3387 | 2.75 | 0.306 | 3605 | 0.675 | 3728 |
| 1400 | 0.500 | 0.219 | 0.000 | — | 0.762 | 3403 | 0.219 | 3400 | 3.49 | 0.256 | 3620 | 0.200 | 3718 |
| 1500 | 0.594 | 0.000 | 0.000 | — | 0.719 | 3403 | 0.094 | 3450 | 7.67 | 0.212 | 3608 | 0.225 | 3710 |

crystalline zircon is well below the level confirmable by our microprobe analyses. Because we are unable to correlate OH band strengths with minor element concentrations, we can only speculate on the assignment of the rest of the bands. It is likely that the bands at ~3420 $cm^{-1}$ (**E∥c**) and ~3385 $cm^{-1}$ (**E⊥c**) correspond to OH at Si-occupied tetrahedral sites. These are the only OH-stretching bands that occur in several of the crystalline zircon samples. Additional OH-stretching bands at ~3270 $cm^{-1}$ (**E⊥c > E∥c**) occur in a few partially metamict zircon samples and may represent differently oriented OH at the vertices of occupied tetrahedra.

The wavenumber and polarization of the OH-stretching bands in crystalline zircon can be used to determine the general environment of the OH groups. In silicate crystals, the H ion of the OH group is usually H bonded to a next nearest neighbor O in the structure. Nakamoto et al. (1955) and Novak (1974) have determined the correlation of OH-stretching band position and O-H···O distance. For H atoms that lie along a linear O-H···O bond, the O···O distance can be estimated. In general, shorter O···O distances produce bands at lower wavenumbers. A fit to Nakamoto's data yields the following approximate O-H···O distances for the zircon OH-stretching mode bands discussed: 3420 $cm^{-1}$ (**E∥c**), 2.87 Å; 3385 $cm^{-1}$ (**E⊥c**), 2.85 Å; 3510 $cm^{-1}$ (**E∥c > E⊥c**), 2.95 Å; and 3270 $cm^{-1}$ (**E⊥c > E∥c**), 2.78 Å.

There are two unique O···O edge distances (two at 2.430 Å and four at 2.752 Å; Robinson et al., 1971) in the $SiO_4$ tetrahedron of zircon. Both are shorter than the inferred O-H···O distances for any of the OH-stretching bands. Because the edges of Si-occupied tetrahedra are too short for the band positions observed, it appears that the H of the OH group may extend outward from the tetrahedron rather than along its edges. This is consistent with the expectation that electrostatic repulsion between Si and H would push the H ion out of the tetrahedron. Electrostatic repulsion would not be a factor at vacant tetrahedral sites, but the inferred O-H···O distance is even greater for the hydrogrossular-type band at 3510 $cm^{-1}$. The discrepancy may decrease if the vacant tetrahedral site expands when Si is not present to counteract the mutual repulsion of the O atoms.

There are two other general environments possible for the H ion outside the silica tetrahedron. One is along the edges of the $[ZrO_8]$ coordination polyhedron, a triangular dodecahedron (Robinson et al., 1971). Again, one would expect electrostatic repulsion to prevent the H from occurring along a polyhedral edge. The second possible location for the H ion is between O atoms that do not share an edge of any occupied polyhedron. There is a vacant sixfold site in the zircon structure with the form of a distorted octahedron that shares faces and edges with both $ZrO_8$ dodecahedra and other vacant octahedra (Robinson et al., 1971). An O-H···O bond between the O atoms that lie on opposite sides of the vacant octahedron would be aligned nearly perpendicular to the c axis, approximately correct for the ~3270 $cm^{-1}$ band. An O-H···O bond between the O atoms that lie along the edge shared by two vacant octahedra would be nearly parallel to the c axis, approximately correct for either the 3420 or ~3510 $cm^{-1}$ bands. Electrostatic repulsion would probably favor such locations because the H ion would point away from the nearest high-valency cations. However, the O···O distance across the vacant octahedron is 3.368 Å, and the shared edge is even longer, much too long to account for the positions of the OH bands observed. Thus, assignment of the OH-stretching modes to particular orientations of the OH group is not straightforward. Perhaps, if the presence of the H ion is the result of a $[M^{3+} + H^+] \leftrightarrow [Zr^{4+}]$ coupled substitution, local distortions of the vacant site caused by the trivalent metal cation's lower charge and (usually) larger ionic radius could affect the O···O distances in a way not accounted for by the average structure determined by X-ray analysis. The ion $Y^{3+}$, for instance, has a radius of 1.02 Å in eightfold coordination (compared to 0.84 Å for Zr) and could cause an adjacent vacant octahedral site to have distances to anions that are smaller than average.

Trace nonstoichiometric substitutions of smaller metal

cations in the normally vacant sixfold site coupled with partial hydroxylation of vacant tetrahedral sites may be another means of incorporating OH into the zircon structure. Our microprobe analyses are not accurate enough to detect such an effect. Finally, metamictization must have a very strong disordering effect on the local environments of OH groups, causing a multitude of sites with a wide range of H-bond strengths and thus broadening the OH bands considerably. Aines and Rossman (1986) have proposed that OH groups act to stabilize the metamict state by terminating broken Zr-O and Si-O bonds. However, our estimates of the amounts of OH in metamict zircon suggest that there is not enough to have a significant effect.

## Conclusions

The only structurally incorporated hydrous species found in zircon is OH. It can be found in zircon of all degrees of crystallinity. Crystalline zircon samples contain 0 to <0.01 wt% OH, expressed as $H_2O$. The highest OH content of any crystalline zircon is in one from the mantle. Metamict and partially metamict zircon samples show a wide range of OH contents, from 0.01 to 0.1 wt%. (Such estimates are subject to revision when accurate calibration of IR data becomes available.) The highest OH content of any partially metamict zircon is in a zircon sample from a hydrothermal vug. The maximum OH content of any of the zircon samples is approximately 2 orders of magnitude less than $H_2O$ contents of radiation-damaged zircon reported in the literature, which were determined by weight loss on heating. It is likely that the greatest fraction of such $H_2O$ was not in fact incorporated in the zircon structure but occurred in cracks and inclusions. All the cyrtolite samples we studied were intergrowths of zircon with other minerals or zircon with abundant secondary inclusions.

The OH-bearing crystalline zircon samples exhibit anisotropic OH bands at ~3420 $cm^{-1}$ ($\mathbf{E} \parallel \mathbf{c}$) and ~3385 $cm^{-1}$ ($\mathbf{E} \perp \mathbf{c}$) resulting from crystallographically oriented OH, possibly at Si-occupied tetrahedra. Such OH may be introduced into the growing crystal by a coupled substitution of the form $[M^{3+} + H^+] \leftrightarrow [Zr^{4+}]$. OH bands at ~3510 $cm^{-1}$ in a few of the crystalline zircon samples result from OH at vacant tetrahedra. This is a much less important OH site in natural zircon than the Si-occupied tetrahedral site. OH may be introduced into that site by the hydrogrossular substitution of the form $[4(OH)^-] \leftrightarrow [(SiO_4)^{4-}]$. Additional OH bands are found at ~3270 $cm^{-1}$. Heating experiments suggest the presence of other stable or metastable OH orientations and demonstrate that labile H can migrate among such sites at elevated temperature.

The various other isotropic bands observed appear to be caused by the presence of randomly oriented hydrous-silicate inclusions distributed throughout the zircon grains or contained in cracks; most notable are the common bands at ~3700 and ~3625 $cm^{-1}$ resulting from the presence of kaolinite.

Partially metamict zircon retains some anisotropy in the OH-stretching region of their spectra. Their OH bands become progressively broader and more asymmetric as metamictization proceeds. The anisotropic band at ~3720 $cm^{-1}$ ($\mathbf{E} \perp \mathbf{c}$) is found in the spectra of only a few partially metamict zircon samples.

Metamict zircon exhibits broad, asymmetric, isotropic OH bands near 3400 $cm^{-1}$. The appearance of such bands results from the multitude of OH sites produced by intense disturbance of the original crystal structure. The highest levels of OH in zircon are found in metamict and partially metamict samples. The actual OH content of some of these samples may be overestimated by a factor of 3 as a result of the presence of kaolinite and fluid inclusions. The sample with the highest primary OH content is a zircon sample from a hydrothermal vug. It is the only crustal zircon with more OH than the kimberlite zircon from the mantle. No other relation to paragenesis can be discerned from our study. Exposure to $H_2O$ during transport may not be an important source of the hydrous species present in alluvial zircon. The discovery of OH-bearing crystalline and partially metamict zircon in this survey indicates that the OH behavior in the widely studied Sri Lanka suite is not representative of all zircon suites.

Further work on additional suites of zircon with known geologic histories and well-characterized U-Th-Pb systematics is required to understand the dependence of OH on paragenesis, metamictization, alteration, annealing, weathering, and alluvial transport. Additional heating, hydrothermal, and deuteration experiments are needed to determine the stability of the OH sites and orientations identified in this study.

## Acknowledgments

This research was funded in part by the Earth Sciences Section, National Science Foundation, grant EAR-7919987 to G.R.R. and Leon T. Silver and grants EAR-8618200 and EAR-8916064 to G.R.R. Leon T. Silver's ongoing interest in the chemistry and behavior of zircon suites of different parageneses was the stimulus for this study. His insight has been highly valuable to us. We thank Armond Chase, Karl Francis, Ed Grew, Warren Hamilton, Anthony Jones, Peter Keller, Demethius Pohl, and Leon Silver for samples included in this work. We thank G. Cleve Solomon for conducting the heating experiment on the Reinbolt Hills zircon sample. Caltech contribution number 4927.

## References cited

Aines, R.D., and Rossman, G.R. (1985) The high temperature behavior of trace hydrous components in silicate minerals. American Mineralogist, 70, 1169–1179.

——— (1986) Relationships between radiation damage and trace water in zircon, quartz, and topaz. American Mineralogist, 71, 1186–1193.

Armstrong, J.T. (1982) New ZAF and a-factor correction procedures for the quantitative analysis of individual microparticles. In K.F.J. Heinrich, Ed., Microbeam analysis—1982, p. 175–179. San Francisco Press, San Francisco.

——— (1988) Quantitative analysis of silicate and oxide materials: Comparison of Monte Carlo, ZAF, and Phi(RhoZ) procedures. In D.E. Newbury, Ed., Microbeam analysis—1988, p. 239–246. San Francisco Press, San Francisco.

Beran, A. (1990) The occurrence of OH absorptions in phenakite—an IR spectroscopic study. Mineralogy and Petrology, 41, 73–79.

Beran, A., and Rossman, G.R. (1989) The water content of nepheline. Mineralogy and Petrology, 40, 235–240.

Beran, A., Rossman, G.R., and Grew, E.S. (1989) The hydrous component of sillimanite. American Mineralogist, 74, 812–817.

Caruba, R., Baumer, A., Ganteaume, M., and Iacconi, P. (1985) An experimental study of hydroxyl groups and water in synthetic and natural zircons: A model of the metamict state. American Mineralogist, 70, 1224–1231.

Chase, A.B., and Osmer, J.A. (1966) Growth and preferential doping of zircon and thorite. Journal of the Electrochemical Society, 113, 198–199.

Coleman, R.G., and Erd, R.C. (1961) Hydrozircon from the Wind River Formation, Wyoming. Journal of Research of the U.S. Geological Survey, 256, 297–300.

Franco, R.R., and Loewenstein, W. (1948) Zirconium from the region of Poças de Caldas. American Mineralogist, 33, 142–151.

Frondel, C. (1953) Hydroxyl substitution in thorite and zircon. American Mineralogist, 38, 1007–1018.

Frondel, C., and Collette, R.L. (1957) Hydrothermal synthesis of zircon, thorite and huttonite. American Mineralogist, 42, 759–765.

Holland, H.D., and Gottfried, D. (1955) The effect of nuclear radiation on the structure of zircon. Acta Crystallographica, 8, 291–300.

Kröner, A., Williams, I.S., Compston, W., Baur, N., Vitanage, P.W., and Perrera, L.R.K. (1987) Zircon ion microprobe dating of high-grade rocks in Sri Lanka. Journal of Geology, 95, 775–791.

Krstanovic, I. (1964) X-ray investigation of zircon crystals containing OH groups. American Mineralogist, 49, 1146–1148.

Lager, G.A., Armbruster, T., Rotella, F.J., and Rossman, G.R. (1989) OH substitution in garnets: X-ray and neutron diffraction, infrared, and geometric-modeling studies. American Mineralogist, 74, 840–851.

Love, G., Cox, M.G., and Scott, V.D. (1978) A versatile atomic number correction for electron-probe microanalysis. Journal of Physics D, 11, 7–27.

Miller, G.H., Rossman, G.R., and Harlow, G.E. (1987) The natural occurrence of hydroxide in olivine. Physics and Chemistry of Minerals, 14, 461–472.

Mumpton, F.A., and Roy, R. (1961) Hydrothermal stability studies of the zircon-thorite group. Geochimica et Cosmochimica Acta, 21, 217–238.

Munasinghe, T., and Dissanayake, C.B. (1981) The origin of gem stones of Sri Lanka, Economic Geology, 76, 1216–1225.

Nakamoto, K., Margoshes, M., and Rundle, R.E. (1955) Stretching frequencies as a function of distances in hydrogen bonds. Journal of the American Chemical Society, 77, 6480–6488.

Newman, S., Stolper, E.M., and Epstein, S. (1986) Measurement of water in rhyolitic glasses: Calibration of an infrared spectroscopic technique. American Mineralogist, 71, 1527–1541.

Novak, A. (1974) Hydrogen bonding in solids. Correlation of spectroscopic and crystallographic data. Structure and Bonding, 18, 177–216.

Özkan, H., Cartz, L., and Jamieson, J.C. (1974) Elastic constants of nonmetamict zirconium silicate. Journal of Applied Physics, 45, 556–562.

Paterson, M.S. (1982) The determination of hydroxyl by infrared absorption in quartz, silicate glasses and similar materials. Bulletin de Minéralogie, 105, 20–29.

Reed, S.J.B. (1965) Characteristic fluorescence corrections in electron-probe microanalysis. British Journal of Applied Physics, 16, 913–926.

Robinson, K., Gibbs, G.V., and Ribbe, P.H. (1971) The structure of zircon: A comparison with garnet. American Mineralogist, 56, 782–790.

Rossman, G.R., and Aines, R.D. (1991) The hydrous components in garnets: Grossular-hydrogrossular. American Mineralogist, 76, 1153–1164.

Rossman, G.R., Beran, A., and Langer, K. (1989) The hydrous component of pyrope from the Dora Maira Massif, Western Alps. European Journal of Mineralogy, 1, 151–154.

Skogby, H., and Rossman, G.R. (1989) $OH^-$ in pyroxene: An experimental study of incorporation mechanisms and stability. American Mineralogist, 74, 1059–1069.

Skogby, H., Bell, D.R., and Rossman, G.R. (1990) Hydroxide in Pyroxene: Variations in the natural environment. American Mineralogist, 75, 764–774.

Woodhead, J.A., Rossman, G.R., and Silver, L.T. (1991) The metamictization of zircon: Radiation dose-dependent structural characteristics. American Mineralogist, 76, 74–82.

Manuscript received September 24, 1990
Manuscript accepted May 23, 1991